LA-UR- 97-2071

Title: Epitaxial $YBa_2Cu_3O_{7-\delta}/Sr_2RuO_4$ Heterostructures

CONF-970302--

Author(s): Darrell G. Schlom, Penn State Univ.
B.A. Merritt, Penn State Univ.
S. Madhavan, Penn State Univ.
Ying Liu, Penn State Univ.
Marilyn E. Hawley, CMS
Geoffrey W. Brown, CMS
A. Dabkowski, McMaster Univ. Canada
H.A. Dabkowski, McMaster Univ.
R. Uecker, Institute fur Krisrallzuchtung Germany
P. Reiche, Institute fur Krisrallzuchtung Germany

Submitted to: Materials Research Society Symposium Proceedings
Epitaxial Oxide Thin Films III 1997

Los Alamos

NATIONAL LABORATORY

Form No. 836 R5
ST 2629 10/91

DISCLAIMER

EPITAXIAL $YBa_2Cu_3O_{7-\delta}$ / Sr_2RuO_4 HETEROSTRUCTURES

D.G. SCHLOM[†], B.A. MERRITT[†], S. MADHAVAN[†], YING LIU[‡], M.E. HAWLEY*, G.W. BROWN*, A. DABKOWSKI[§], H.A. DABKOWSKA[§], R. UECKER[◊], AND P. REICHE[◊]

[†] Department of Materials Science and Engineering, Penn State University, University Park, PA 16802-5005, schlom@ems.psu.edu

[‡] Department of Physics, Penn State University, University Park, PA 16802

*Center for Materials Science, Los Alamos National Laboratory, Los Alamos, NM 87545

[§] Institute of Materials Research, McMaster University, Hamilton, Ontario, Canada L8S 4M1

[◊] Institut für Kristallzüchtung, 12489 Berlin, Germany

ABSTRACT

The anisotropic oxide superconductors $YBa_2Cu_3O_{7-\delta}$ and Sr_2RuO_4 have been epitaxially combined in various ways (*c*-axis on *c*-axis, *c*-axis on *a*-axis, and *a*-axis on *a*-axis) though the use of appropriate substrates. Phase-pure *a*-axis oriented or *c*-axis oriented epitaxial Sr_2RuO_4 films were grown by pulsed laser deposition. $YBa_2Cu_3O_{7-\delta}$ films were then grown on both orientations of Sr_2RuO_4 films and the resulting epitaxy was characterized.

INTRODUCTION

Sr_2RuO_4 is unique in several respects. It is the only known layered perovskite that is free of copper, yet superconducting. Single crystals exhibit superconductivity below a transition temperature (T_c) of 1.35 K [1-3]. Among all known perovskites, layered or not, Sr_2RuO_4 is the only one which exhibits superconductivity without any intentional doping. Superconductivity is only seen in very pure single crystals and not in polycrystalline samples. Paramagnetic impurity levels of 400 ppm are sufficient to destroy superconductivity in this compound [3]. Finally, Sr_2RuO_4 is believed to exhibit an unconventional *p*-wave pairing symmetry [4].

The excellent lattice match of Sr_2RuO_4 with $YBa_2Cu_3O_{7-\delta}$ makes it an attractive candidate for use as a normal metal in superconductor—normal metal—superconductor (*SNS*) Josephson junctions or as epitaxial electrodes to $YBa_2Cu_3O_{7-\delta}$. Chemical compatibility between Sr_2RuO_4 and $YBa_2Cu_3O_{7-\delta}$ is expected because several cuprate superconductors are known that contain RuO_6 octahedra in close proximity to CuO_2 planes, e.g., $RuSr_2ReCu_2O_8$ and $RuSr_2(Re_{1+x}Ce_{1-x})Cu_2O_{10}$, where *Re* is one of the rare-earth atoms Sm, Eu, or Gd [5]. For example, the compound $RuSr_2ReCu_2O_8$ [5] may be thought of as a superlattice consisting of a [CuO_2-*Re*-CuO_2] cuprate block (the center portion of the $ReBa_2Cu_3O_{7-\delta}$ unit cell) followed by a Sr_2RuO_4 formula unit (half a unit cell), stacked on top of each other along the *c*-axis.

The properties of Sr_2RuO_4 and $SrRuO_3$ (the endpoints of the $Sr_{n+1}Ru_nO_{3n+1}$ Ruddlesden-Popper homologous series) are compared in Table I. The electronic and magnetic properties of this homologous series are unusual. The $n = 1$ member of this series, Sr_2RuO_4, contains perovskite sheets connected in two dimensions and is paramagnetic (above $T_c \approx 1.35$ K). The neighboring ($n = 2$) compound, $Sr_3Ru_2O_7$, is ferromagnetic ($T_c = 104$ K) [6]. At the other end of the series ($n = \infty$) lies the three-dimensionally connected perovskite $SrRuO_3$, which is also ferromagnetic ($T_c = 160$ K). In addition to its potential for device applications, $YBa_2Cu_3O_{7-\delta}$ / Sr_2RuO_4 heterostructures may be useful for studying the proximity coupling between these oxide superconductors which may have very different pairing symmetries.

TABLE I: Properties of Sr_2RuO_4 and $SrRuO_3$ [7-9].

Barrier Material Orientation (*hkℓ*)	Lattice Constants at 25 °C (Å)	α (10^{-6}/°C)	Resistivity at 77 K (Ω·cm)	Lattice Mismatch to $YBa_2Cu_3O_7$ (001)
$SrRuO_3$ (110)	$a = 5.532$ $b = 5.572$ $c = 7.850$		9×10^{-5}	2.7 % (*a*) 1.1 % (*b*)
Sr_2RuO_4 (001)	$a = 3.870$ $c = 12.74$	18 (*a*) 6.5 (*c*)	1.4×10^{-5} (*a,b*) 3×10^{-2} (*c*)	0.5 %

EXPERIMENTAL

Sr_2RuO_4 and $YBa_2Cu_3O_{7-\delta}$ films were grown by on-axis pulsed laser deposition (PLD) from stoichiometric targets. The Sr_2RuO_4 films were grown on (100) $LaAlO_3$, (110) $NdGaO_3$, and (100) $SrTiO_3$ (for *c*-axis films) and on (100) $LaSrGaO_4$ and (100) $LaSrAlO_4$ (for *a*-axis films) at a substrate temperature of 1000 °C, an oxygen background pressure of 2×10^{-6} Torr, a KrF (λ = 248 nm) laser fluence of 2 J/cm^2, a pulse rate of 2-50 Hz, and cooled in vacuum. A radiative heater allowed the substrates to be heated to temperatures as high as 1090 °C [10]. Further details on the Sr_2RuO_4 target synthesis, film growth, and pressure-temperature conditions in which the Sr_2RuO_4 phase is stable during PLD growth are given elsewhere [11,12]. The $YBa_2Cu_3O_{7-\delta}$ films were grown by 90° off-axis PLD at substrate temperatures from 650-800 °C, an oxygen/ozone (~5% ozone) pressure of 20 mTorr, a KrF laser fluence of 2 J/cm^2, a pulse rate of 50 Hz, and cooled in 0.5-1 atmosphere of oxygen. For the growth of $YBa_2Cu_3O_{7-\delta}$ / Sr_2RuO_4 heterostructures, the chamber was vented between layers to switch between on-axis and off-axis PLD geometries and to switch targets. The Sr_2RuO_4 films were heated in vacuum and the oxygen/ozone background pressure was introduced just before the initiation of the $YBa_2Cu_3O_{7-\delta}$ growth to avoid degradation of the Sr_2RuO_4. For some growths a $Sr_{1.2}Ba_{0.8}RuO_4$ target was used with the same growth conditions as used for Sr_2RuO_4. The (100) $LaSrGaO_4$ and (100) $LaSrAlO_4$ substrates were grown by the Czochralski method as described elsewhere [13,14].

The films were characterized using a Picker 4-circle x-ray diffractometer, a Nanoscope III scanning tunneling microscope (STM), and 4-point resistance versus temperature measurements.

RESULTS AND DISCUSSION

c-axis Sr_2RuO_4 *on (100)* $LaAlO_3$*, (110)* $NdGaO_3$*, and (100)* $SrTiO_3$

Single-phase epitaxial Sr_2RuO_4 films have been grown on the {100} plane of the perovskite subcell of common perovskite substrates: $LaAlO_3$, $NdGaO_3$, and $SrTiO_3$. As expected from lattice matching considerations, the Sr_2RuO_4 grows with its *c*-axis oriented normal to the {100} plane of the perovskite subcell of these substrates (*c*-axis oriented), as illustrated in Fig. 1. X-ray diffraction scans of a ~1000 Å thick Sr_2RuO_4 film grown on a (100) $SrTiO_3$ substrate are shown in Fig. 2. Together these scans indicate that the film grows with the orientation relationship depicted in Fig. 1. The full width at half maximum (FWHM) of the Sr_2RuO_4 x-ray peaks in all angles (2θ, ω, and ϕ) is comparable to the instrumental resolution of our Picker 4-circle x-ray diffractometer equipped with a flat graphite incident beam monochrometer. Resistivity versus temperature measurements reveal that the as-grown Sr_2RuO_4 films are metallic, but not superconducting [15].

The surface of this same Sr_2RuO_4 film was imaged with scanning tunneling microscopy (STM) and is shown in Fig. 3. The surface morphology revealed by STM is highly dependent on the misorientation of the substrate. The image shown is for a film grown on a well-oriented (100) $SrTiO_3$ substrate (misorientation ≤ 0.2°). More vicinal substrates result in surfaces stepped in the direction of misorientation, indicating that the growth occurs by step-propagation.

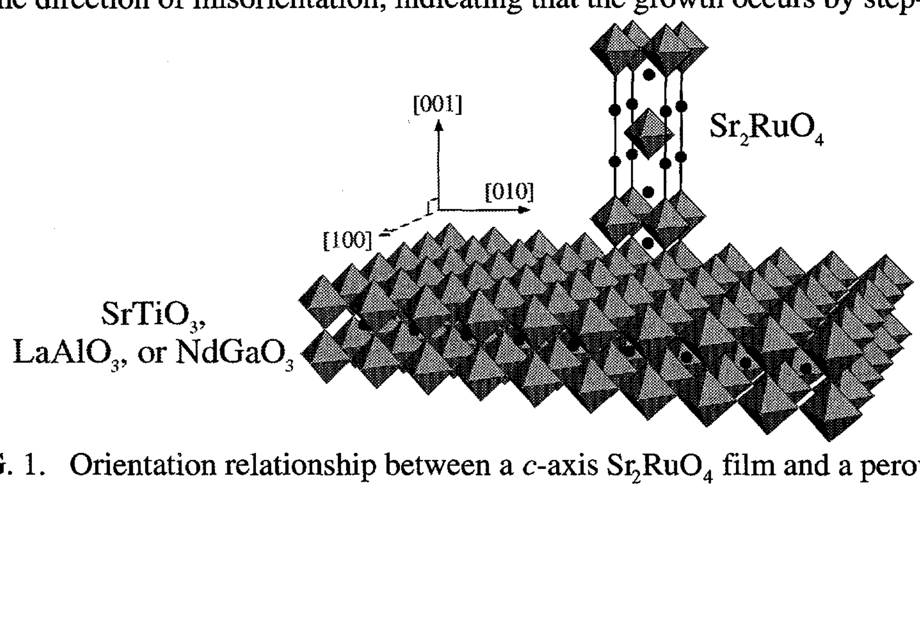

FIG. 1. Orientation relationship between a *c*-axis Sr_2RuO_4 film and a perovskite substrate.

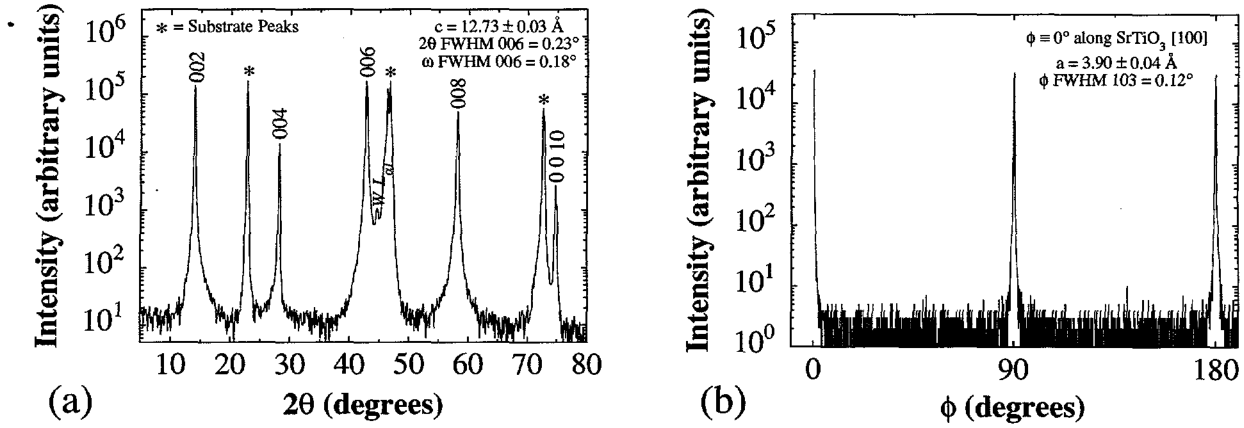

FIG. 2. (a) θ-2θ x-ray diffraction scan and (b) 103 peak x-ray diffraction ϕ-scan of a *c*-axis Sr_2RuO_4 film grown on (100) $SrTiO_3$.

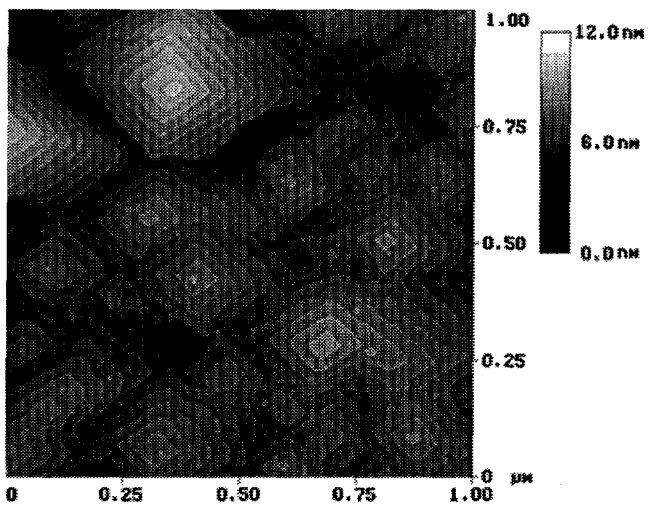

FIG. 3. STM image of the surface of a *c*-axis Sr_2RuO_4 film grown on (100) $SrTiO_3$.

a-axis Sr_2RuO_4 on (100) $LaSrGaO_4$ and (100) $LaSrAlO_4$

Single-domain *a*-axis Sr_2RuO_4 films have been grown on (100) $LaSrGaO_4$ and (100) $LaSrAlO_4$ substrates. These substrate materials are isostructural with Sr_2RuO_4 and the orientation relationship shown in Fig. 4 is expected from lattice match considerations. As the x-ray diffraction patterns in Fig. 5 indicate, this is indeed the orientation adopted by the epitaxial Sr_2RuO_4 films. The peaks every 180° (2-fold symmetry) in the ϕ-scan indicate that the Sr_2RuO_4 film is single-domain. A small amount (<0.1% by volume) of *c*-axis Sr_2RuO_4 is also present in the film, giving rise to the 00 ℓ Sr_2RuO_4 peaks.

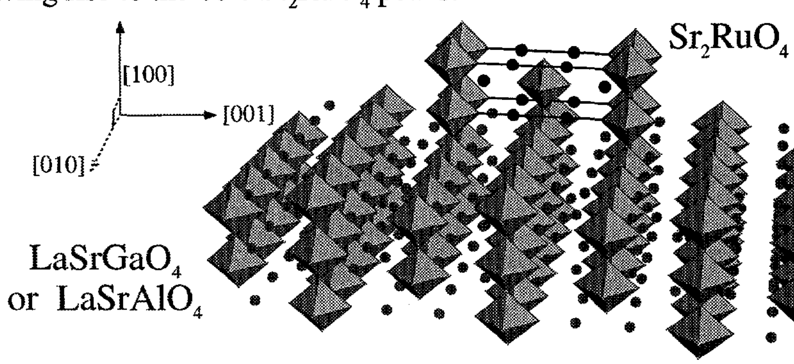

FIG. 4. Orientation relationship between a (100) $LaSrGaO_4$ or (100) $LaSrAlO_4$ substrate and an *a*-axis oriented Sr_2RuO_4 film. Note the 2-fold rotational symmetry about the axis perpendicular to the substrate (the [100] axis) of this epitaxial arrangement.

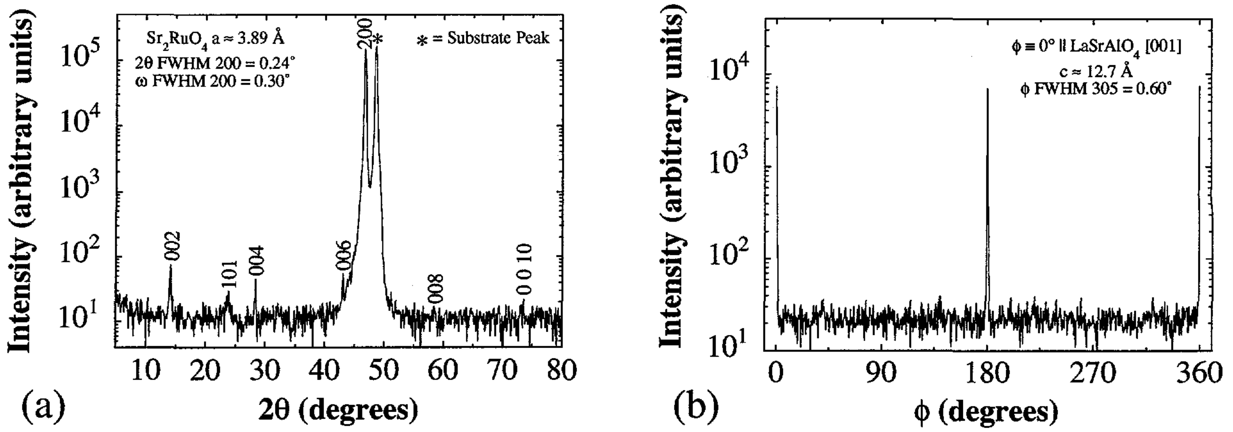

FIG. 5. (a) θ-2θ x-ray diffraction scan and (b) 305 peak x-ray diffraction φ-scan of an *a*-axis Sr_2RuO_4 film grown on (100) $LaSrAlO_4$.

$YBa_2Cu_3O_{7-\delta}$ on Sr_2RuO_4

We recently reported the epitaxial growth of *c*-axis $YBa_2Cu_3O_{7-\delta}$ films on *c*-axis oriented Sr_2RuO_4 films on (100) $LaAlO_3$ with T_c (of the $YBa_2Cu_3O_{7-\delta}$) of 92 K [16]. This observation is consistent with the good transport properties measured for *c*-axis $YBa_2Cu_3O_{7-\delta}$ films grown on the cleaved (001) faces of Sr_2RuO_4 single crystals [9]. Here we report the growth of $YBa_2Cu_3O_{7-\delta}$ films on *a*-axis $(Sr,Ba)_2RuO_4$ films on (100) $LaSrGaO_4$. Similar to the growth

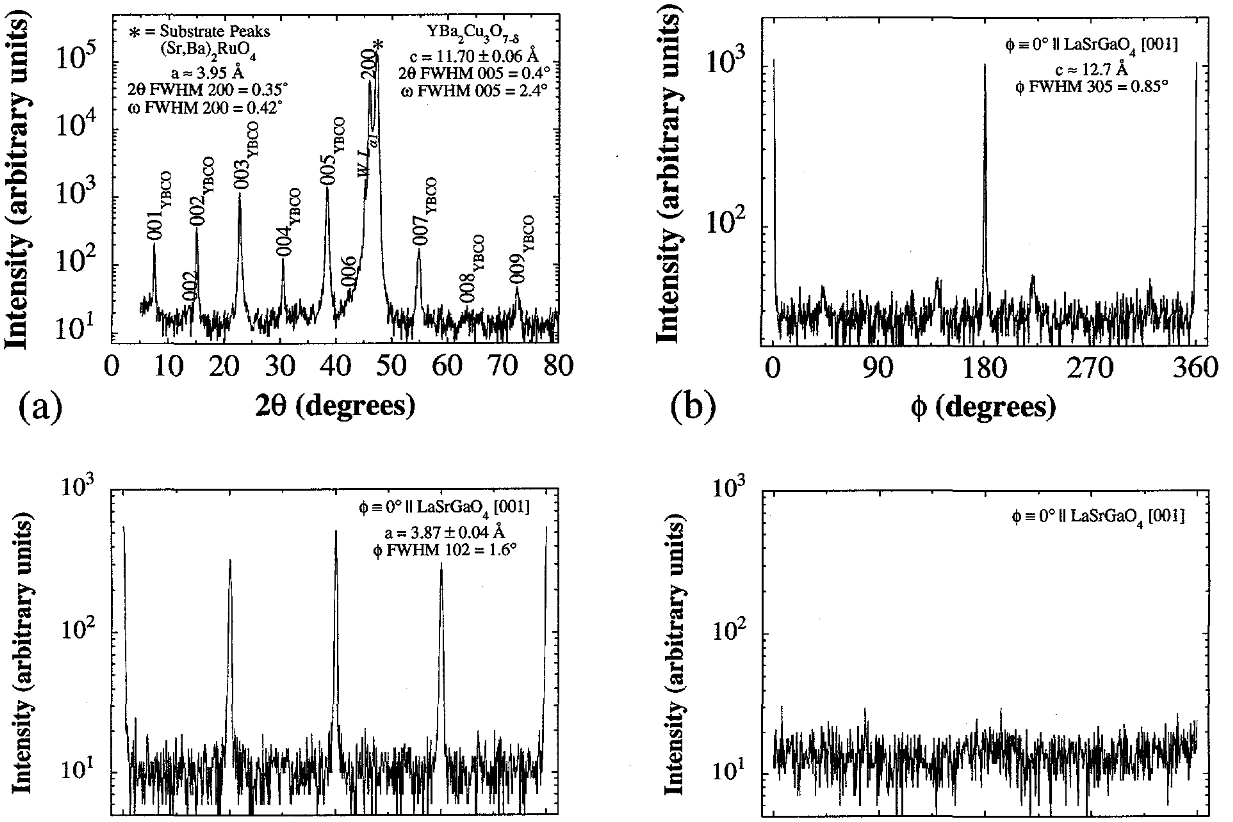

FIG. 6. (a) θ-2θ x-ray diffraction scan, (b) 305 peak x-ray diffraction φ-scan of underlying *a*-axis $(Sr,Ba)_2RuO_4$ film grown on (100) $LaSrGaO_4$, (c) 102 peak x-ray diffraction φ-scan of overlying *c*-axis $YBa_2Cu_3O_{7-\delta}$ film grown on *a*-axis $(Sr,Ba)_2RuO_4$, and (d) 102 peak x-ray diffraction φ-scan of overlying *a*-axis $YBa_2Cu_3O_{7-\delta}$ film grown on *a*-axis $(Sr,Ba)_2RuO_4$.

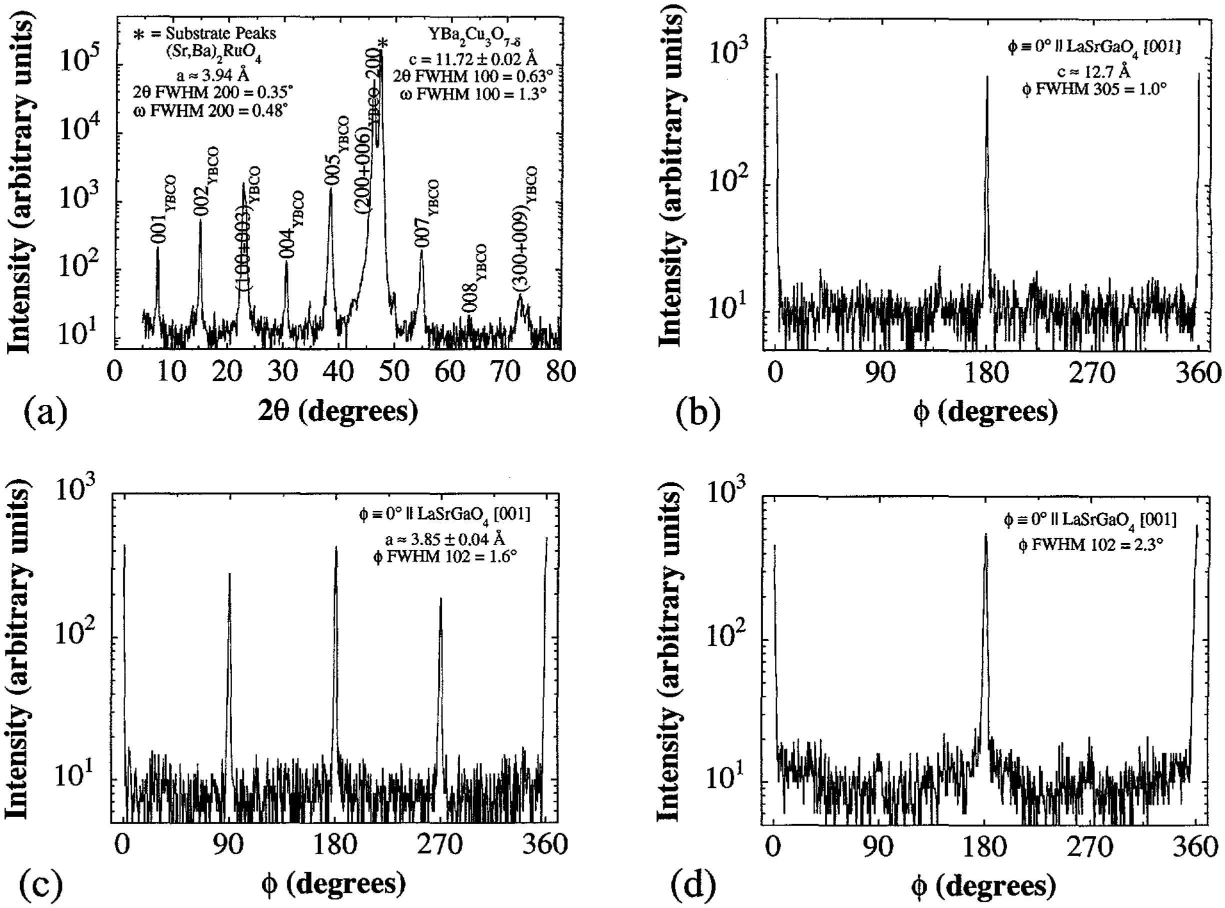

FIG. 7. (a) θ-2θ x-ray diffraction scan, (b) 305 peak x-ray diffraction ϕ-scan of underlying *a*-axis (Sr,Ba)$_2$RuO$_4$ film grown on (100) LaSrGaO$_4$, (c) 102 peak x-ray diffraction ϕ-scan of overlying *c*-axis YBa$_2$Cu$_3$O$_{7-\delta}$ film grown on *a*-axis (Sr,Ba)$_2$RuO$_4$, and (d) 102 peak x-ray diffraction ϕ-scan of overlying *a*-axis YBa$_2$Cu$_3$O$_{7-\delta}$ film grown on *a*-axis (Sr,Ba)$_2$RuO$_4$.

orientation of YBa$_2$Cu$_3$O$_{7-\delta}$ on other materials (e.g., on bare (100) LaSrGaO$_4$ substrates [17,18]), at high growth temperatures the YBa$_2$Cu$_3$O$_{7-\delta}$ films are *c*-axis oriented, at low temperatures they are *a*-axis oriented, and at intermediate growth temperatures mixed orientation is observed.

Figure 6 shows the x-ray diffraction patterns of a YBa$_2$Cu$_3$O$_{7-\delta}$ film grown at high substrate temperature (T_{sub} ≈ 800 °C). The YBa$_2$Cu$_3$O$_{7-\delta}$ film is epitaxial and entirely *c*-axis oriented. At lower growth temperature (see Fig. 7), the YBa$_2$Cu$_3$O$_{7-\delta}$ film is of mixed *a*-axis and *c*-axis orientation (but mainly *a*-axis oriented). Note that the in-plane orientation of the *a*-axis YBa$_2$Cu$_3$O$_{7-\delta}$ grown on *a*-axis (Sr,Ba)$_2$RuO$_4$ is untwinned with complete in-plane alignment of the *c*-axes of the films with each other and with the substrate, i.e., the orientation relationship is:

(100) YBa$_2$Cu$_3$O$_{7-\delta}$ ∥ (100) (Sr,Ba)$_2$RuO$_4$ ∥ (100) LaSrGaO$_4$ and

[001] YBa$_2$Cu$_3$O$_{7-\delta}$ ∥ [001] (Sr,Ba)$_2$RuO$_4$ ∥ [001] LaSrGaO$_4$.

This untwinned orientation relationship is identical to that seen for the growth of *a*-axis YBa$_2$Cu$_3$O$_{7-\delta}$ on other substrates with the K$_2$NiF$_4$ structure, i.e., (100) LaSrGaO$_4$, (100) LaSrAlO$_4$, and (100) Nd$_2$CuO$_4$ [18]. However, unlike these other materials with the K$_2$NiF$_4$ structure, (Sr,Ba)$_2$RuO$_4$ is conductive.

CONCLUSIONS

YBa$_2$Cu$_3$O$_{7-\delta}$ and Sr$_2$RuO$_4$ films may be epitaxially integrated in various ways: *c*-axis on *c*-axis, *a*-axis on *a*-axis, and *c*-axis on *a*-axis. All three of these orientation relationships were achieved through the use of an appropriate substrate giving the desired Sr_2RuO_4 film orientation and appropriate growth conditions for the $YBa_2Cu_3O_{7-\delta}$ overlayer to influence whether it grows *c*-axis oriented (high T_{sub}) or *a*-axis oriented (low T_{sub}). Phase-pure epitaxial Sr_2RuO_4 films were first grown. Single-domain *c*-axis Sr_2RuO_4 films were grown on (100) $LaAlO_3$, (110) $NdGaO_3$, and (100) $SrTiO_3$ substrates. Single-domain *a*-axis Sr_2RuO_4 epitaxial films were grown on (100) $LaSrGaO_4$ and (100) $LaSrAlO_4$ substrates. Epitaxial $YBa_2Cu_3O_{7-\delta}$ films were then grown on Sr_2RuO_4 films with each of these orientations. Due to the high substrate temperatures required to grow epitaxial Sr_2RuO_4 films, it is not possible to grow the Sr_2RuO_4 layer on top of the $YBa_2Cu_3O_{7-\delta}$ layer by PLD.

ACKNOWLEDGMENTS

We gratefully acknowledge the financial support of the National Science Foundation through grant DMR-9357614.

REFERENCES

1. Y. Maeno, H. Hashimoto, K. Yoshida, S. Nishizaki, T. Fujita, J.G. Bednorz, and F. Lichtenberg, Nature **372**, 532 (1994).

2. Y. Maeno and K. Yoshida, Czech. J. Phys. **46**, 3097 (1996).

3. Y. Maeno, presented at the 1997 March Meeting of the American Physical Society in Kansas City, MO 1997 (unpublished).

4. T.M. Rice and M. Sigrist, J. Phys. Condens. Matter **7**, L643 (1995).

5. L. Bauernfeind, W. Widder, and H.F. Braun, Physica C **254**, 151 (1995).

6. G. Cao, S. McCall, and J.E. Crow, Phys. Rev. B **55**, R672 (1997).

7. R.J. Bouchard and J.L. Gillson, Mater. Res. Bull. **7**, 873 (1972).

8. J.S. Gardner, G. Balakrishnan, and D.McK. Paul, Physica C **252**, 303 (1995).

9. F. Lichtenberg, A. Catana, J. Mannhart, and D.G. Schlom, Appl. Phys. Lett. **60**, 1138 (1992).

10. J.C. Clark, J.P. Maria, K.J. Hubbard, and D.G. Schlom, to be published in Rev. Sci. Instrum.

11. S. Madhavan, D.G. Schlom, A. Dabkowski, H.A. Dabkowska, and Y. Liu, Appl. Phys. Lett. **68**, 559 (1996).

12. S. Madhavan, Y. Liu, D.G. Schlom, A. Dabkowski, H.A. Dabkowska, Y. Suzuki, I. Takeuchi, Z. Trajanovic, and R.P. Sharma, to be published in IEEE Trans. Appl. Supercond.

13. A. Dabkowski, H.A. Dabkowska, and J.E. Greedan, J. Cryst. Growth **132**, 205 (1993).

14. A. Gloubokov, R. Jablonski, W. Ryba-Romanowski, J. Sass, A. Pajaczkowska, R. Uecker, and P. Reiche, J. Cryst. Growth **147**, 123 (1995).

15. Y. Liu, J.A. Mitchell, S. Madhavan, D.G. Schlom, A. Dabkowski, and H.A. Dabkowska, Czech. J. Phys. **46**, 1113 (1996).

16. S. Madhavan, J.A. Mitchell, T. Nemoto, S. Wozniak, Y. Liu, D.G. Schlom, A. Dabkowski, and H.A. Dabkowska, to be published in J. Cryst. Growth.

17. S. Hontsu, N. Mukai, J. Ishii, T. Kawai, and S. Kawai, Appl. Phys. Lett. **61**, 1134 (1992).

18. S. Miyazawa and M. Mukaida, Appl. Phys. Lett. **64**, 2160 (1994).